COMMUNICATION

ChemComm
www.rsc.org/chemcomm

Electrodeposition of monodispersed Fe nanocrystals from an ionic liquid

C. L. Aravinda† and W. Freyland*

Institute of Physical Chemistry, University of Karlsruhe (TH), Kaiserstrasse 12, D-76128 Karlsruhe, Germany. E-mail: Werner.Freyland@chem-bio.uni-karlsruhe.de; Fax: +49-721-608-6662; Tel: +49-721-608-2100

Received (in Cambridge, UK) 1st July 2004, Accepted 4th September 2004
First published as an Advance Article on the web 19th October 2004

Monodispersed Fe nanocrystals up to ~2 nm thick, ~50 nm wide and ~120 nm long have been electrodeposited from the ionic melt $AlCl_3$–1-methyl-3-butylimidazolium chloride {$AlCl_3$–$[MBIm]^+Cl^-$} at room temperature on Au(111) and have been characterized *in-situ* by electrochemical scanning tunneling microscopy.

Nanostructures possess unique properties due to size and interface effects and hence find many applications in electronics, catalysis, and material science.[1] Various techniques now permit the production of nanostructures, making it possible to tailor the properties of the materials for specific functionalities. Electrochemical methods are among the most viable ones to prepare metal nanostructures which allow the precise control over grain size by adjusting the electrochemical parameters such as overpotential, current density and the bath composition. Electrochemical scanning tunneling microscopic (EC-STM) studies on the spontaneous formation and growth of metal nanostructures from aqueous electrolytes in the sub-micron range have been reported, see *e.g.* refs. 2–4. However, electrodeposition from aqueous solutions is restricted to potential ranges where water is not reduced. Hence most of these investigations where aqueous electrolytes have been employed are limited to electrodeposition of elements more noble than hydrogen. Recently, electrodeposition of nanocrystalline metals from room-temperature molten salt electrolytes for various functional applications has been highlighted.[5] In this communication we report a novel procedure to electrodeposit monodispersed Fe nanocrystals on Au(111) by employing a room-temperature acidic molten salt electrolyte $AlCl_3$–$[MBIm]^+Cl^-$ and, for the first time, have characterized them by *in-situ* EC-STM monitoring the two-dimensional (2D) phase formation and three-dimensional (3D) growth of Fe nanocrystals.

Fig. 1 shows the cyclic voltammogram of different redox processes on Au(111) of an $AlCl_3$–$[MBIm]^+Cl^-$ (58:42) melt containing 5 mM Fe(II).‡ Starting from the onset of Au bulk oxidation at the anodic limit of 1.9 V, the redox couple A/A′ at 1.8 V refers to Au oxidation at the step edges of the Au substrate.[6] A small reduction wave at 0.6 V is due to the UPD of Al on Au(111) which is described in detail in our EC-STM studies on underpotential deposition of Al (UPD) on Au(111) form the same melt.[7] In agreement with the previous electrochemical studies[8] in $AlCl_3$–BuPyCl, the reduction wave C near 0.4 V is assigned to Fe deposition in the OPD range, as is evidenced by the STM and XPS results shown below. The reduction wave D at 0.25 V and a steep increase in reduction current (E) beyond the Nernst potential, respectively, are assigned to the Fe–Al co-deposition and Al bulk deposition.

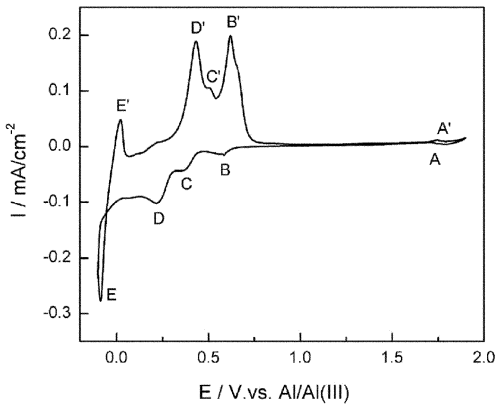

Fig. 1 Cyclic voltammogram of an ionic melt {$AlCl_3$–$[MBIm]^+Cl^-$} + 5 mM Fe(II) on Au(111) recorded with a sweep rate of 0.05 V s^{-1} at 294 K.

The *in-situ* EC-STM experiments were carried out using a home-built scanning tunneling microscope driven by a Picoscan controller (Molecular Imaging Co., USA).§ At the beginning of the EC-STM experiments, a clear surface of Au(111) with steps of monoatomic height was observed at an open circuit potential (OCP) of 1.5 V. Few nuclei on the terraces and also along the step edges were seen due to the UPD of Al (see ref. 7) at an applied potential of 0.6 V (STM picture not shown). No further deposition and growth of clusters was seen at this potential even after a duration of 120 min. When the potential was further reduced to 0.42 V, after about 4 min 2D islands, presumably of Fe, grew on the Au(111) terraces (Fig. 2(a)). Initially these islands grew very slowly in the direction parallel to the step edges and formed elongated islands as shown in the STM image (Fig. 2(b)) scanned after 20 min. Height profile analysis for the successive STM images obtained at 2 min intervals revealed that these islands grew two-dimensionally and also three-dimensionally to several monolayer thicknesses, unlike UPD of metal islands, which is limited to 2D growth up to 1–2

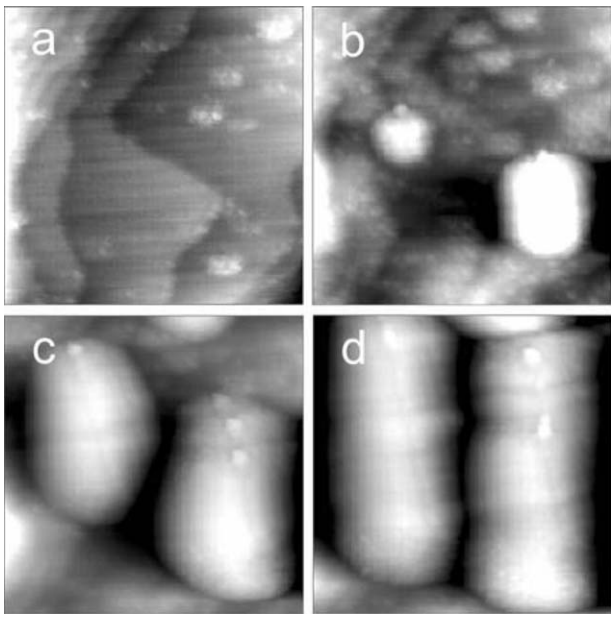

Fig. 2 Representative STM images (125 × 125 nm^2) showing the initial stages of nucleation and the growth of Fe nanocrystals on Au(111): (a) 4 min, (b) 26 min, (c) 30 min and (d) 34 min; E = 0.42 V, E_{tip} = 0.52 V, I_{tunn} = 1 nA.

† *Present address*: Physik Department – E19, Techn. Universität München. E-mail: aravinda@ph.tum.de

DOI: 10.1039/b409861g

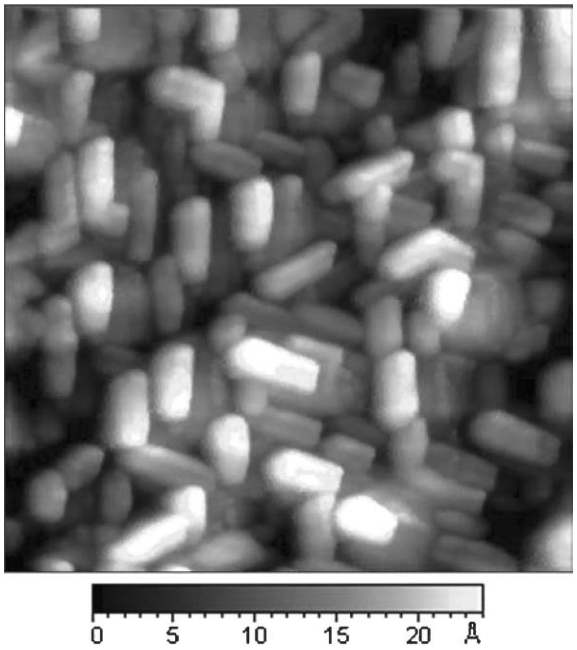

Fig. 3 STM image (160 × 160 nm^2) of monodispersed Fe nanocrystals. E = 0.4 V, E_{tip} = 0.7 V, I_{tunn} = 1 nA.

monolayers. The islands continue to grow with time but do not coalesce, instead they grow rapidly in length rather than in width to form individual nanocrystal domains (Fig. 2(c)). Each nanocrystal reaches a uniform width of about 50 nm and a length of about 120 nm (Fig. 2(d)). The average height of such nanocrystals is ~2 nm. Typically grown monodispersed Fe nanocrystals on Au(111) by stepping the potential directly from OCP to 0.4 V are shown in Fig. 3. Some of the crystals align in boomerang shapes with an angle of about 120–140° like self-ordered Fe nanostructures on Si(111).[9] The latter have been prepared by rf-sputtering and so the formation mechanism of the Fe nanostructures may be different. The nanocrystals prepared under these conditions are remarkably stable up to an anodic potential of 0.8 V.

In order to confirm the deposition of Fe, XPS spectra for a sample deposited on Au(111) potentiostatically at 0.4 V for 10 min were recorded using Al–Kα radiation (1486.6 eV) in a chamber housing the OMICRON EA 125 multichannel hemispherical analyzer. In the spectra (Fig. 4) of an as-prepared sample a weak peak at 707 eV and a broad hump at 711.1 eV due to Fe and FeO_x are observed. Upon sputtering the sample for 5 min with an Ar^+ ion beam, the Fe $2p_{3/2}$ peak becomes more prominent. There is no shift in the binding energy of the Fe $2p_{3/2}$ peak which confirms the deposition of pure Fe.[10] The peak seen for FeO_x is due to surface oxidation of the sample while transferring from the glovebox to the XPS spectrometer. Trace signatures of Al and chloride were also seen in the spectra of as-prepared samples which almost vanish upon sputtering. This could originate from spurious adsorbed electrolyte.

Results of our *in-situ* EC-STM studies show, for the first time, that monodispersed Fe nanocrystals can be electrodeposited from an ionic melt $AlCl_3$–$[MBIm]^+Cl^-$ on Au(111). Such nanocrystals with well defined shape open further perspectives for nanotechnological applications. The acidic molten salt electrolyte $AlCl_3$–$[MBIm]^+Cl^-$ used in the present studies has a large electrochemical window of greater than 2 V *vs.* Al/Al(III) on Au(111) and certainly opens an arena for electrochemical synthesis of a new class of nanostructured materials. In comparison to aqueous electrolytes it has a specific advantage that hydrogen evolution does not interfere with the nucleation and growth of deposits. In-depth studies on the potential dependent growth kinetics and efforts to tailor the crystal size are underway.

Financial support of this study by the DFG Center of Functional Nanostructures, University of Karlsruhe, is acknowledged. C. L. A thanks the Alexander-von-Humboldt foundation for a fellowship.

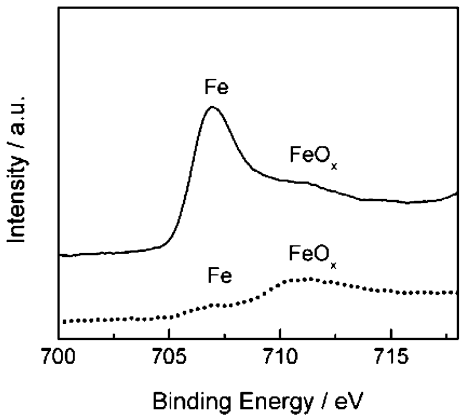

Fig. 4 XPS spectra of Fe nanocrystals deposited on Au(111) at 0.4 V from an ionic melt {$AlCl_3$–$[MBIm]^+Cl^-$} + 5 mM Fe(II); (– – –) before sputtering, (—) after 5 min sputtering.

Notes and references

‡ The method used to synthesize $[MBIm]^+Cl^-$ from 1-ethylimidazole and 1-chlorobutane (Merck) and the purification by recrystallization have been described earlier.[11] Anhydrous $AlCl_3$ (Fluka, >99%) was purified by adding 2 mass% of NaCl and 0.2 mass% of Al and heating this mixture in an evacuated quartz ampoule up to 200 °C for several hours followed by the distillation of $AlCl_3$. The $AlCl_3$ crystals were slowly added to $[MBIm]^+Cl^-$ in a molar ratio of 58:42. Fe(II) was introduced into the {$AlCl_3$–$[MBIm]^+Cl^-$} melt by controlled potential-coulometric dissolution of an Fe wire (Alfa, >99.99%, 0.25 mm) up to a concentration of 5 mM. All the above processes were carried out under high purity argon atmosphere. § A detailed description of the specially designed home-built electrochemical STM setup used in the present investigations is given in ref. 12. A pre-cleaned Teflon electrochemical cell (effective area of 0.36 cm^2) with three-electrode assembly was used for all the studies. In every experiment a fresh gold sample (12 × 12 mm^2, Berliner Glas KG, Germany) was annealed in an H_2 flame and cooled slowly in a N_2 stream prior to use as a working electrode. An Fe ring and Al wire (>99.99%, Alfa Acer, Germany) dipped in to the melt served as the counter and reference electrode, respectively. The STM tips were freshly prepared by etching tungsten wires (250 μm diameter, >99.98%, Alfa) in a NaOH solution (2 mol l^{-1}). To avoid the effect of Faraday currents, tips were coated *via* electrophoresis with an electropaint (BASF ZQ 84-3225 0201, Germany) and cured at 150 °C for 2 h and subsequently at 200 °C for 10 min. The whole setup for the EC-STM studies was assembled in an argon-filled glovebox (O_2 and H_2O < 1 ppm) and mounted in a clean and Ar-filled airtight stainless steel container to ensure relatively long measurement times.

1 *Frontiers in Surface and Interface Science*, ed. C. B. Duke and E. W. Plummer, Elsevier, Amsterdam, 2002.
2 F. A. Moller, O. M. Magnussen and R. J. Behm, *Phys. Rev. Lett.*, 1996, **77**, 5249.
3 H. Hagenstrom, M. A. Schneeweiss and D. M. Kolb, *Langmuir*, 1999, **15**, 7802.
4 Y. Gimeno, A. Hernandez, P. Carro, S. Gonzalez, R. C. Salvarezza and A. J. Arvia, *J. Phys. Chem. B*, 2002, **106**, 4232.
5 F. Endres, M. Bukowski and R. Hempelmann, *Angew. Chem., Int. Ed.*, 2003, **42**, 3428.
6 C. A. Zell, F. Endres and W. Freyland, *Phys. Chem. Chem. Phys.*, 1999, **1**, 697.
7 C. L. Aravinda, I. Mukhopadhyay and W. Freyland, *Phys. Chem. Chem. Phys.,* in press.
8 M. Lipsztajn and R. A. Osteryoung, *Inorg. Chem.*, 1985, **24**, 716.
9 M. Cougo dos Santos, J. Geshev, D. K. Silva, J. E. Schmidt, L. G. Pereira, R. Huber and P. Allongue, *J. Appl. Phys.*, 2003, **94**, 1490.
10 A. Velon and I. Olefjord, *Oxid. Met.*, 2001, **56**, 425.
11 F. Endres and W. Freyland, *J. Phys. Chem. B*, 1998, **102**, 10229.
12 A. Shkurankov, F. Endres and W. Freyland, *Rev. Sci. Instrum.*, 2002, **73**, 102.